



## Experimental Investigation and Numerical Prediction of Fatigue Life in Force Fitted Fastener Holes

Hadi Taghizadeh\*, Tajbakhsh Navid Chalherlou

*Department of Mechanical Engineering, University Of Tabriz, Tabriz, 51666-14766, Iran*

(Manuscript Received --- 31 May 2017; Revised --- 24 Dec. 2017; Accepted --- 11 Mar. 2018)

### Abstract

In this paper, the effect of interference fit on fatigue life of holed plate of mechanical joints was investigated experimentally. Fatigue tests were carried out on the holed specimens of Al-alloy 7075-T6 alloy. The interference fit process consists of force fitting a fastener into the hole with a negative clearance (diameter of the fastener is larger than of the hole) that produces beneficial tangential pre-stress at the edge of the hole. Stress and strain analysis was implemented in order to estimate the fatigue life due to interference fit process. 3D finite element simulations have been performed to obtain stress and strain histories and distributions around the hole due to interference fit and subsequent cyclic longitudinal loading using ANSYS package. The results obtained from the finite element analysis of the interference fit were employed to predict the fatigue life. The fatigue life was divided into two phases of crack initiation life and fatigue crack growth life. Fatigue initiation life was estimated using Fatemi–Socie multiaxial fatigue criterion, and the fatigue crack growth life was predicted using AFGROW computer code. The results show that there is a good agreement between the numerically predicted total fatigue life and experimental fatigue test results.

*Keywords:* Interference Fit, Fatigue Life, Finite Element, Crack Initiation Life, Crack Growth Life.

### 1- Introduction

Bolted joints, as part of mechanically fastened joints, are the most common structural joints in the commercial airplanes and aerospace structures. These joints are used despite their drawbacks, because of their low cost and simplicity of assembling. With increasing in the testing and experimentation of the structural materials, it becomes apparent that the majority of fatigue found in the aerospace structures was located at specific components' regions where there are bolt holes, grooves and other notches. These areas exhibit a dramatic decrease in fatigue

life during test due to an increased stress as a result of stress concentration. This stress concentration eventually causes early fatigue crack initiation and propagation. There are many methods of inducing pre-stress and residual stress to improve fatigue life in mechanical parts, including shot peening, surface cold rolling, tensile overloading, use of interference fit fasteners, low plasticity burnishing, laser shock peening, coining around holes and cold expansion of holes [1-5].

The interference fit process expands the fastener hole diameter to create a pre-stress field around the hole. This process refers to

a fastener which has larger diameter than the hole of the fastener. Interference fit fasteners increase the fatigue life of a component, as they maintain the shape of the hole, impeding deformation and strain from loading. Interference fit is easily applied to a number of components because it only requires access to one side of the hole. Care must be taken, however, to track the entrance and exit side of the mandrel as the pre-stress field is not uniform through the thickness, and induces P shape crack fronts [6].

Fatigue damage is among the major issues in engineering; this damage increases with the number of applied loading cycles in a cumulative manner, and can lead to fracture and failure of the engineering components. Therefore, the prediction of fatigue life has an outstanding importance that must be considered during the design step of a mechanical component [7].

In the estimation of fatigue life two stages are usually distinguished: a crack initiation and the subsequent crack propagation, which are the results of different mechanisms. Several approaches have been proposed to calculate the fatigue life in mechanical components in a variety of conditions. The first group is based on the models which consider the crack nucleation phase only, using a combination of damage evolution rule based on the stress/strain of components. The key points of these models are being independent from loading and specimen geometry. The main fatigue damage occurs on the critical plane, which is based on the physical observations, i.e. fatigue cracks initiate and grow within a material on certain planes, where the growth and orientation depend on the stresses and strains in these planes. Brown and Miller [8] suggested the

combined use of maximum shear strain range and tensile strain normal to the plane of the maximum shear. Based on the magnitudes of stresses, strains or a combination of both, some multi-axial criteria are used to predict fatigue life, such as Ruiz Criterion [9], Shear Stress Rang (SSR) [10], McDiarmid parameter [11] and Crossland criterion [12] which are based on the stress criteria, and Smith–Watson–Topper (SWT) parameter [13] which includes both stress and strain components. Fatemi and Socie criterion [14] considers maximum shear strain amplitude and maximum normal stress acting on the maximum shear strain plane. However, all of these criteria are employed to predict the total lifetime of the structures instead of calculating the contributions of crack initiation and crack propagation. In contrast, the other approach considers the propagation phase as the whole of the process, in view of a number of existing factors such as the geometry or the high stress levels and the assumption of previously existing defects in the shape of microcracks, e.g. cracks that are initiated from an inclusion in the very first load cycles [15, 16]. Toyosada et al. [17] proposed a new driving force parameter by considering the effect of cyclic plastic zone near the crack tip. A recent model known as “NASGRO Equation” was developed by NASA [18]. The proposed model examines fatigue crack growth (FCG) by accounting the mean stress effect and the plasticity induced crack closure phenomenon. The model’s ability for predicting FCG rate and FCG life was proved through a comparison study with experimental data [19, 20]. Recently, and due the fact that the plastic zone around the crack tip has a significant effect on the fatigue crack growth rate, Li et al. [21, 22] developed an analytical

solution to account the influence of the plastic deformation during cyclic loading. Thus, a plasticity-induced stress intensity factor expression was given under small-scale yielding conditions. To predict crack growth life some computer programs such as AFGROW, NASGROW and FASTRAN codes can be utilized [23, 24]. In recent years, some approaches have been proposed to predict the total life as the combination of the number of cycles necessary to initiate a crack,  $N_i$ , and the number of cycles required to propagate this crack until failure,  $N_p$  [25]. In these approaches fatigue crack initiation and propagation lives are estimated separately, then the total fatigue life is calculated by adding them [26].

The objective of the present study is to investigate the fatigue behavior of interference fitted holes and also estimation fatigue life of the specimens using a numerical method. Fatigue behaviors that have been studied include both fatigue life and fatigue crack initiation location. For this purpose fatigue tests were conducted on the samples made of Al-alloy 7075-T6. The specimens were classified into two batches of Open hole (OH) and Interference Fitted (IF) specimens. In conjunction with the fatigue tests, finite element (FE) method was used to simulate the interference fit process and the subsequent remote cyclic loading. The stress and strain fields obtained from the finite element analysis were employed to estimate the fatigue life of the specimens. The fatigue life was divided into two phases of fatigue initiation life and fatigue crack propagation life. The initiation life was estimated by using Fatemi–Socie multiaxial fatigue criterion using the stress and strain fields obtained from the FE

simulations. Incorporating the FE solutions into AFGROW computer program, the resulting stress intensity factor (SIF) and fatigue crack propagation life were calculated. The predicted lives were compared with the experimental test results.

## 2- Experimental procedures

The specimen configuration used in this research, shown in Fig.1. Fatigue test specimens were cut from an Al-alloy 7075-T6 plate with dimensions of 1.25m×1.25m×6.35mm. The samples longitudinal axes were positioned along the plate rolling direction. Then a central hole was made in samples by drilling and reaming. The 400, 800 and 1000 mesh number emery papers were used for polishing and removing the surface scratches.

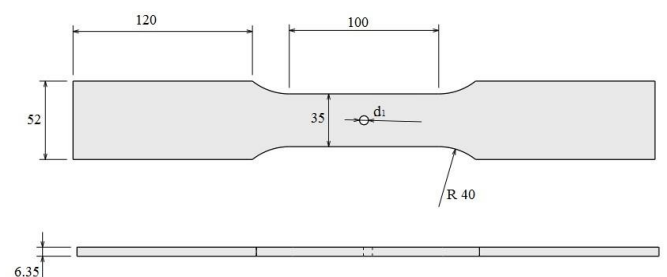


Fig. 1 Fatigue test specimen (mm).

To conduct interference fit process, a bolt with a bigger diameter than that of the hole was inserted into the fatigue specimen. To implement the interference fit, the force fitting of the bolt into the specimens' hole was carried out with a hydraulic test machine, as shown in Fig. 2. On the machine lower jaw, a steel cylindrical support, with a central hole, was used underneath the specimens. The steel cylinder had a central hole with diameter of 10 mm and 1 mm chamfer (at its hole edge), and an outer diameter of 35mm. The steel bolts inserted into fatigue specimen

were M6 class 12.9. The used bolts were half threaded with the shank diameter of 5.90 mm where the threaded parts were machined to reach the diameter of 5.4 mm and it was made tapered having a 15° chamfer (slope) between the shank and the threaded region by machine. The fatigue specimens' hole diameters were  $d_1 = 5.9$  and 5.7mm, so the interference sizes of IF = 0% (open hole), and 3.5% were created during the bolt insertion. The most important parameter in the interference fit process is the interference fit size that can be defined as follow:

$$IF = \frac{d_2 - d_1}{d_1} \times 100 \quad (1)$$

where  $d_2$  is the bolt shank diameter and  $d_1$  is the hole diameter.

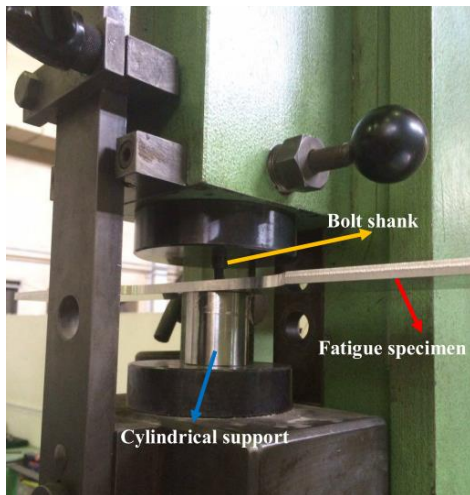


Fig. 2 Interference fit set up.

An electro-hydraulic fatigue testing machine (Zwick/RoellAmsler) with a maximum load capacity of 500 kN have been used for the fatigue tests. The stress ratio and frequency in the fatigue test were  $R = \sigma_{\min}/\sigma_{\max} = 0.1$  and 4 Hz respectively in all tests. The specimen was mounted on the fatigue testing machine as represented in Fig. 3. After fatigue test, the life, the

number of load cycles until specimen failure, at the applied cyclic load ranges have been recorded and displayed in S-N diagram (Fig. 4).

Based on the established curves, it is clearly evident that the interference fit process significantly improves the fatigue life of the specimens and IF specimens endure longer fatigue life (life until final fracture of the specimen) compared to the specimens including only open hole. The interference fit (IF) increases fatigue life by a factor from 2 to 8, depending on the level of applied fatigue stress.



Fig. 3 Test specimen mounted on the fatigue test machine

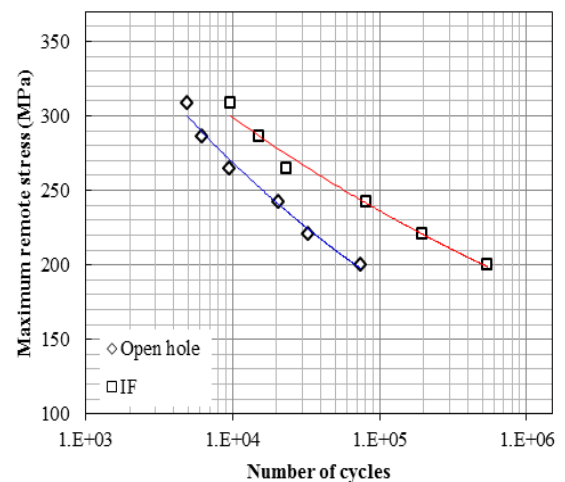


Fig. 4 Fatigue test results

To have a better view on the fatigue test results and the effect of interference fit on the fatigue crack initiation location and propagation region, the fracture section of the specimens were thoroughly examined. Fig. 5 show the fatigue crack initiation location and fatigue crack growth region at the smallest cross-section of the specimens subjected to the loads of 50 kN and 70 kN. The fracture sections exhibit that at the open hole specimens fatigue cracks are initiated at the mid plane for all loads. As Fig. 5 demonstrates the fatigue cracks are initiated at the entrance plane for the interference fitted specimens.

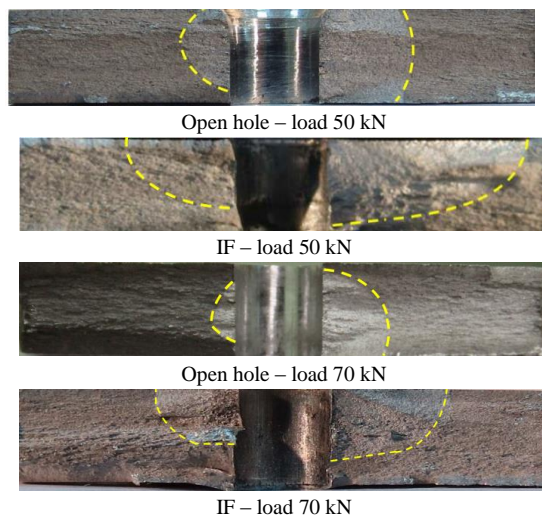


Fig. 5 Fracture section of the specimens.

### 3. Numerical stress and strain analyses

Three-dimensional (3-D) finite element (FE) models [27] were used to simulate the interference fitting process and the subsequent cyclic loading to obtain the local stress and strain distributions around the fastener hole. Because of the symmetry of the load and the geometry with respect to X-Z and Y-Z planes in the specimens, only a quarter of these specimens were modeled. The dimensions of the experimental specimens were used to build the FE models. The 3D structural brick elements, as called SOLID185 in ANSYS,

were used for the 3D modelling of the bolt and plate. This cubic-shaped element has eight nodes, and each having three degrees of freedom (translations in the x, y, and z directions). The use of these elements provides the same accuracy in plasticity ( $2 \times 2 \times 2$  integration points) as the higher-order elements (20-node element), but requires much less computational time to converge the numerical solutions, especially in nonlinear problems such as a contact analysis [27].

Contact between the components of bolted joints is a main feature that transfers the applied load or contact pressure among the contacting components in the joints. Therefore, it is essential to model contact conditions accurately in the bolted joints in order to achieve much more reliable results. Contact problems are generally classified into two classes: rigid-to-flexible and flexible-to-flexible. Bolted joints are an example of flexible-to-flexible contact problems as in the joints the plates and the bolt are allowed to be deformed. ANSYS can model contact problems with contact elements based on the Lagrange multiplier, penalty function, and direct constraint approach. During meshing a model, the nodes on the potential contacting surfaces comprise a layer of contact elements which their four Gauss integration points are used as contacting checkpoints. ANSYS provides three contact models: node-to-node, node-to-surface, and surface-to-surface. Each type of contact model uses a different set of ANSYS contact elements and is appropriate for specific types of problems. Contact in the bolted joints is addressed using these contact types and their elements depending on the model being used. For the solid 3D modelling, the surface-to-surface contact is mostly used.

For the FE model of the bolted joint, a 3D surface-to-surface contact element CONTA174 was used to represent the contact between contacting surfaces in the joint model [27]. A 3D target segment element TARGE170 was also used to associate with CONTA174 via a shared real constant set.

These contact elements allow the pressure to be transferred between the pin and the plate at the hole surfaces, but without them penetrating into each other. The 3-D finite element mesh of the fatigue specimens is demonstrated in Fig. 6.

In the finite element models material properties are required. Linear elastic with multi-linear kinematic hardening plasticity material relationship was used to represent the Al- alloy 7075-T6. A true stress-strain diagram for the Al- alloy 7075-T6 was obtained from a simple tensile test. The stress-strain behavior of the material is shown in Fig. 7. In the figure the stress-strain behavior of the aluminum plate (Al-alloy 7075-T6) was obtained from simple tensile tests in the rolling direction. The steel bolt was assumed to have an elastic modulus of 207 MPa and yield strength high enough to preclude yielding. Poisson's ratio was taken as 0.33 for plate and 0.29 for the bolt shank.

The FE solution was conducted in three load steps. In the first load step, the pin was placed inside the hole to simulate the interference fitting process. To constrain the pin and plate in the model, symmetric displacement boundary condition was applied to the symmetry planes. The pin was also constrained in its central nodes to avoid rigid body motion. By incrementing the position of nodes' on the pin upper face in the  $-Z$  direction, with the total

displacement of  $U_z = -10$  mm, the simulation of interference fit was performed.

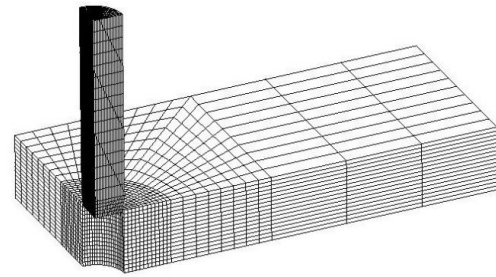


Fig. 6 Finite element of model.

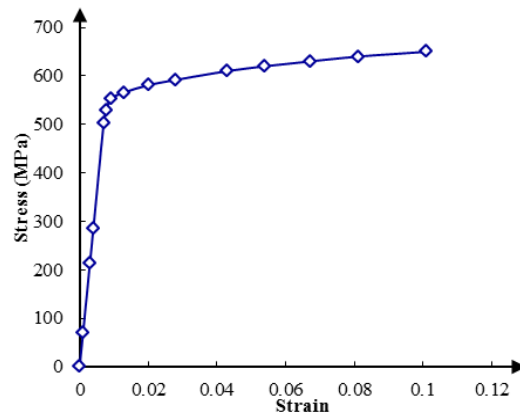


Fig. 7 Stress-strain curve of Al- alloy 7075-T6.

In the next stage, the cyclic longitudinal loading was applied in a quasi-static way along the longitudinal axis at the end of the plate away from the hole. In this stage a remote stress was incrementally increased from the minimum value to its maximum value (loading) at the end of plate and then it was decreased incrementally to its minimum value (unloading). It is necessary to mention that the loading and unloading stages were repeated two cycles to consider the changes in the stress and strain distributions occurring after plastic deformation at the first load cycle.

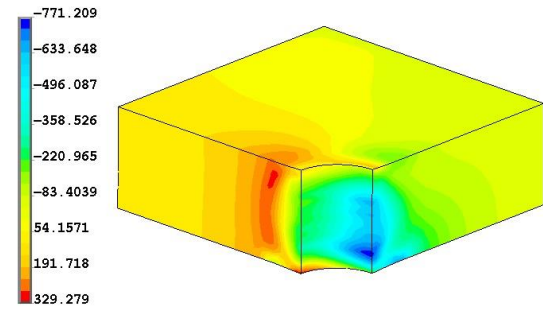
#### 4. Results and discussion

##### 4.1. Stress results for IF model and cyclic loading

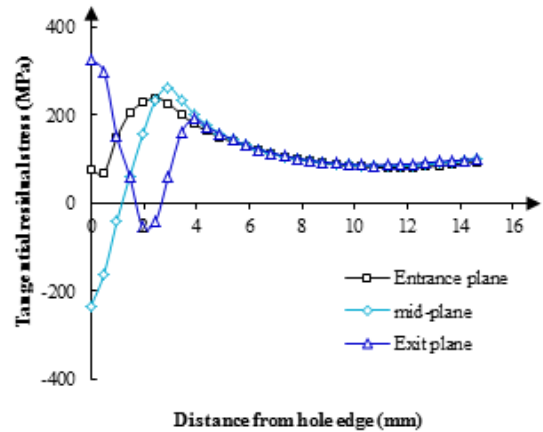
The fatigue life improvement considerably depends on the pre-stress distribution surrounding the hole. The tangential pre-

stress distribution of the interference fit at the entrance, mid and the exit planes is displayed in Fig 8. It can be seen that the pre-stress produced by interference fit at the entrance and exit planes are tensile, however, it is compressive in the mid plane. The different stress states and incremental insertion of the bolt result in non-uniform pre-stress distribution through the plate thickness during the interference fit process. Due to low material constraint on the entrance and exit planes, the state of stress in these regions is in plane stress condition. Consequently, it is not surprising that the level of the pre-stress generated by hole interference fit around the entrance and exit planes is different from the mid-plane where the state of plane strain condition is prevailed. For this reason, the pre-stress generated by interference fit inherently has a non-uniform distribution through the plate thickness. On the other hand, plastic flow of the material along the pin travelling direction during the expansion process provokes more reduction in the material constraint on the entrance plane and leads to increase of that on the mid-plane and the exit plane.

In order to consider the distribution of the resultant stresses around the hole, when the plate is subjected to cyclic loads in the presence of the interference fitted pin, a longitudinal remote tensile stress in X-direction was subsequently applied to the end of the plate after IF process. The effect of remote loading and subsequent unloading of the plate on the tangential pre-stress distribution was obtained in the forms of mean and amplitude stresses at the plate net section. These stresses were calculated based on the following concept [28]:



(a)



(b)

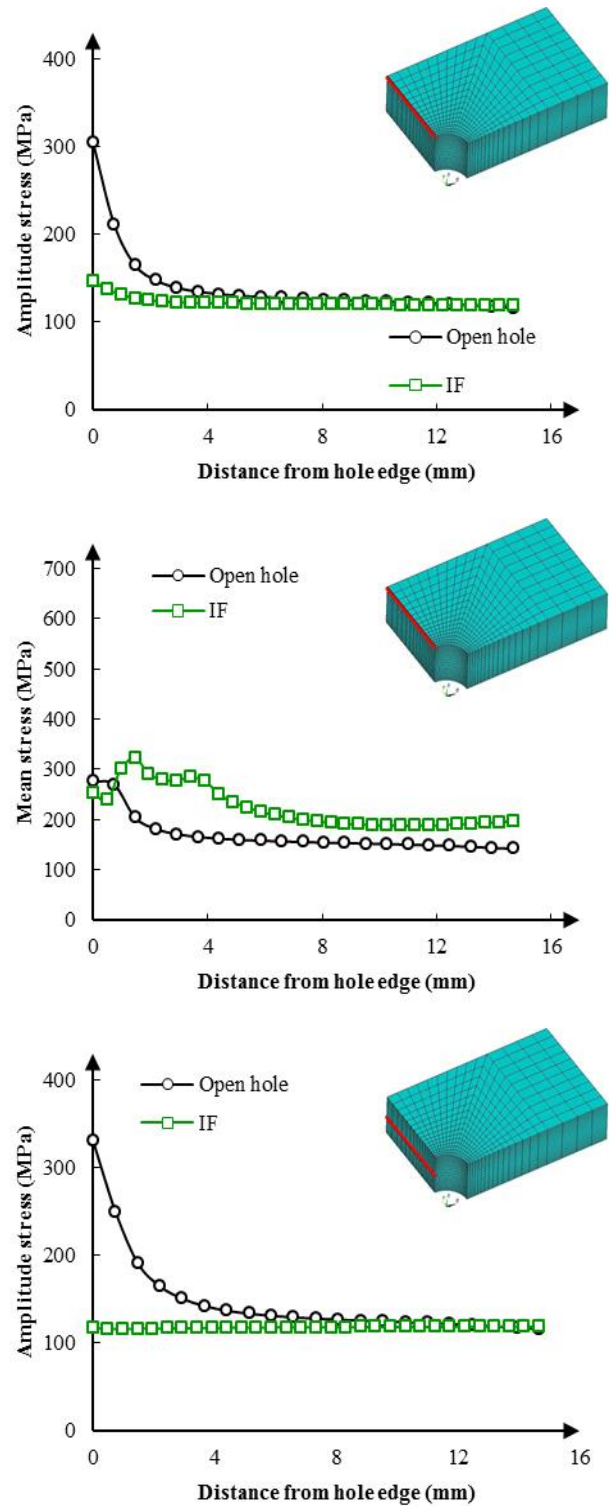
Fig. 8 (a) Tangential pre-stress (MPa) contour plot for IF 3.5 %. (b) Distributions of tangential pre-stress in X-direction result in the interference fit

$$\sigma_a = \frac{\sigma_{\max} - \sigma_{\min}}{2} \quad (2)$$

$$\sigma_m = \frac{\sigma_{\max} + \sigma_{\min}}{2} \quad (3)$$

Where  $\sigma_a$  is the local tangential amplitude stress,  $\sigma_m$  is the local tangential mean stress,  $\sigma_{\max}$  is the maximum local tangential stress and  $\sigma_{\min}$  is the minimum local tangential stress. The distribution of amplitude and mean stresses on the entrance plane, mid-plane and exit plane are displayed in Fig. 9 typically for maximum remote stress of 265 MPa (i.e. load 60 kN). Interference fit process creates beneficial pre-stresses nearby the hole. The beneficial pre-stress created by the interference fit process may cause a mean stress rise at some distance from the hole edge, but it significantly reduces the

stress amplitude in the specimens near the hole edge. The stress amplitude decrease is beneficial in postponing the initiation of fatigue crack and retarding fatigue crack propagation, therefore, increasing the fatigue life. As Fig. 9 displays at interference fitted specimens, stress amplitude substantially decreases in comparison with the open hole specimen on the entrance, mid and exit planes. The mean stress profile is more complex than the amplitude stress profile. In the interference fitted specimens the mean stress rises on the exit plane, but decreases on the entrance and mid-plane. The reduction of mean stress distribution is more considerable on the mid plane. This figure describes that the stress amplitude is larger on the mid-plane at the open hole edge. Likewise, the mean stress value is also bigger on the same location compared to the other surface-planes at the hole edge of open hole models which confirm the observed crack initiation location at the fractured sections (see Fig. 5). In the interference fitted specimens, the stress amplitude and mean stress are considerably lower in the mid-plane compared to the entrance plane. This proves that in the interference fitted specimen fatigue crack initiation is more likely to occur near the entrance edge. This is in accord with the experimental results.



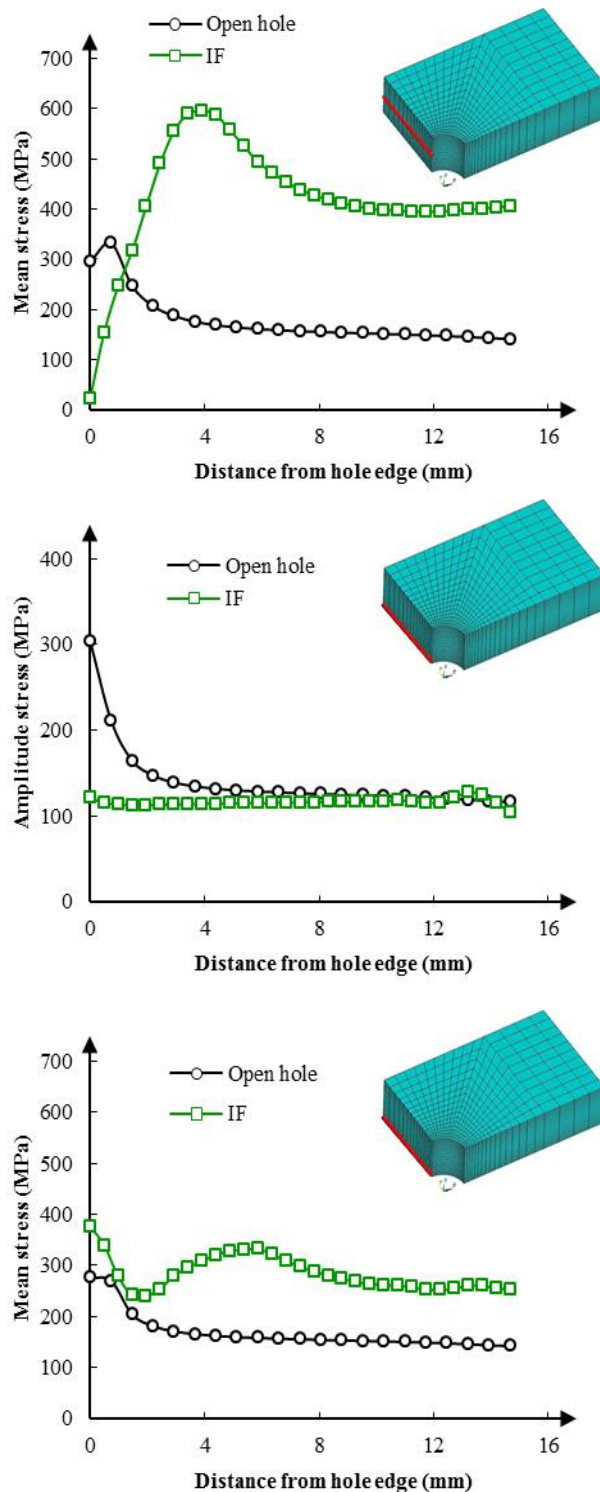


Fig. 9 The distribution of stress amplitude  $\sigma_a$  and the mean stress  $\sigma_m$  distributions (in X-direction) at 60 kN load.

Based on the experimental and the FE simulation, fatigue life improvement of IF specimens has been attributed to: (1) beneficial tangential pre-stresses created by the interference fit process that reduces

the magnitude of the stress amplitude around the hole, (2) considerable contact pressure between the bolt shank and the hole surface that can carry a part of the applied load and (3) reduced stress concentrations.

#### 4.2. Fatigue crack initiation phase

The initiation phenomenon begins by nucleation of a crack at the region of maximum stress and strain (near the hole). Stress state in the vicinity of the hole is multiaxial, and non-proportional owing to the interference fit and cyclic longitudinal loading. Due to the complexity of the stress field, a multiaxial fatigue criterion must be employed. To predict fatigue crack initiation life, there are many well-known multi-axial fatigue criteria such as Smith–Watson–Topper (SWT) [13], Kandil, Brown and Miller (KBM) [8] and Fatemi–Socie (FS) [14]. In ductile materials (e.g. Al-alloy 7075T-6) fatigue cracks typically nucleate along the slip systems, which are aligned with the maximum shear planes. Since the material used in this paper is ductile, so a criterion with shearing failure mode dominant would be proper one. Fatemi–Socie model considers maximum shear strain amplitude and maximum normal stress acting on the maximum shear strain plane. In this work, the well-known Fatemi–Socie (FS) [14] criterion is used, though other multiaxial criteria can also be applied. The FS parameter is based on the range of shear strain  $\Delta\gamma_{\max}$  on the critical plane, i.e. the plane where the maximum  $\Delta\gamma$  is produced. The parameter is defined as [14]:

$$\frac{\Delta\gamma_{\max}}{2} \left( 1 + k \frac{\sigma_n^{\max}}{\sigma_y} \right) = (1+\nu) \frac{\sigma_f^2}{E} (2N_f)^b + \frac{k}{2} (1+\nu) \frac{\sigma_f^2}{E} (2N_f)^{2b} + 1.5\varepsilon_f' (2N_f)^c + \frac{k}{2} 1.5 \frac{\sigma_f' \varepsilon_f'}{E} (2N_f)^{b+c} \quad (4)$$

where the material dependent constants of fatigue properties are given in Table 1.  $\sigma_y$  is the material yield strength,  $k$  is a material constant which can be found by fitting fatigue data from uniaxial tests to fatigue data from pure torsion tests,  $\sigma_f'$  is the fatigue strength coefficient,  $b$  is the fatigue strength exponent,  $\varepsilon_f'$  is the fatigue ductility coefficient,  $c$  is the fatigue ductility exponent, and  $E$  is the modulus of elasticity. The maximum normal stress on the maximum shear strain plane,  $\sigma_n^{\max}$  takes constitutive behavior into account including additional hardening due to the non-proportionality of loading. The critical plane for this model is identified as the plane experiencing the maximum shear damage parameter  $\left( \frac{\Delta\gamma_{\max}}{2} \left( 1 + k \frac{\sigma_n^{\max}}{\sigma_y} \right) \right)$  and the fatigue life is estimated based on the accumulated damage on this plane.

**Table 1** fatigue life coefficient [18]

The material constant	$\sigma_y$ (MPa)	$\sigma_f'$ (MPa)	$\varepsilon_f'$	$b$	$c$
	503	1446	0.262	-.143	-.619

#### 4.3. Initial crack shape and dimensions

The important parameter in calculating the fatigue crack propagation life is the initial crack length. For this purpose the initial crack size, crack shape and location of

crack initiation should be specified. The fractured sections of the interference fitted specimens show that the fatigue crack was initiated from the hole edge at the entrance plane at the net section and it propagated quarter-elliptically form at the both side of the hole, and at the open hole specimens crack was initiated at the mid plane and it propagated semi-elliptically form at the both side of the hole. For more clarity, the initial crack geometry can be seen in both directions in Fig 10.

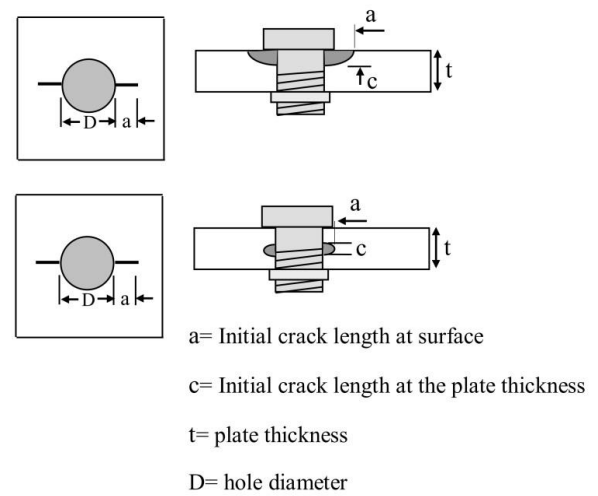


Fig. 10 Initial crack shape and nomination.

There are different techniques to detect the minimum crack length such as Liquid penetrant, Ultrasonic and Radiography (X-ray/Gamma ray) [28]. Many researchers agree that the initial crack length is between 0.25 and 0.5 mm for notched samples [29]. For engineering analysis the initial crack size is usually considered  $0.127 \text{ mm}$  [30]. In this work an initial flaw size of  $L_{ci}=0.1 \text{ mm}$  was assumed at the surface for all interference fitted specimens. This number was chosen as it is near to the initial flaw size of the mechanically fastened aluminum joints studied by Dhamari [30]. The ratio  $(L_a / L_c)$  will be about 0.5. So in this research  $L_a$  was assumed to be 0.05mm.

#### 4.4. Crack propagation

It is believed that when a pin is interference fitted in a fastener hole, it will open the existing crack (i.e. pre-crack or fatigue crack), creating a non-zero stress intensity factor in the absence of an externally applied load. Even though the magnitude of the maximum stress intensity factor after the application of cyclic loads will increase, the SIF range ( $\Delta K_I = K_{I_{max}} - K_{I_{min}}$ ) will be lower compared to the case with no interference fit under cyclic loading. This reduction in stress intensity factor range will result in slower crack growth rates. AFGROW code was developed by Harter [18] based on the concept of linear elastic fracture mechanics (LEFM). The crack propagation life estimation was implemented using the material properties, specimen's dimensions and test conditions. To obtain the fatigue crack growth life, a plate was employed in AFGROW using the classic model of double quarter elliptical crack at the hole in the entrance plane of the pin under far-field cyclic loading. The dimensions entered in AFGROW code have the same dimensions of the test specimen. Fatigue cracks were assumed to be originated at  $\theta=90^\circ$ , i.e. at the smallest cross sectional area.

To simulate the effect of longitudinal loading, the spectrum option in AFGROW code was used to provide a means of specifying the load/stress spectrum. In this option, the loading is assumed to be far-field loading. This means that the remote load is applied at the end of the plate where the effect of stress concentration is very small. The walker crack growth law was used to predict crack propagation rate,  $da/dN$  in the following form [28]:

$$\frac{da}{dN} = c \left[ \Delta K (1-R)^{m-1} \right]^n \quad (5)$$

where  $da/dN$  is the crack growth rate,  $\Delta K$  is the applied stress-intensity factor range,  $R$  is the stress ratio and  $C, m, n$  are empirical constants, which are obtained by curve fitting the test data.

In order to calculate the stress intensity factors due to pre-stresses, AFGROW computer code was employed. The AFGROW computer code includes an option that users can simply input the known pre-stress distributions through a dialog window. There are two methods available in the AFGROW to calculate the stress intensity factors due to residual stresses or pre-stresses. They are the Gaussian integration and the weight function method. The Gaussian integration method was used in this study. For this purpose, the pre-stress profile that obtained from the FE simulation was introduced in a table provided by the code as a function of the crack length in the plate thickness and surface directions to the AFGROW to include the interference fit effect on the crack growth rate and fatigue crack growth life.

#### 4.5. Estimation of total fatigue life

The total fatigue life of the interference fitted specimens that subjected to different constant amplitude remote stresses (applied loads) was predicted. The life was predicted with a method that combines initiation and propagation lives. The number of cycles to crack initiation ( $N_i$ ) was calculated using FS criterion and the number of cycles to crack growth until the final fracture ( $N_p$ ) was evaluated using walker equation. The total fatigue life ( $N_t=N_i + N_p$ ) is obtained by adding the

initiation life and the propagation life of a crack from the initiation length to the final fracture.

The fatigue crack initiation life ( $N_i$ ) was shown in Fig. 10. As the figure shows the fatigue crack initiation life for the interference fitted specimens is bigger than the open hole specimens. In the interference fitted specimens the initiation life is improved. This is related to fact that the stress concentration factor is lower in the interference fitted specimens than the open hole specimens. The influence that an interference-fit has on the stress concentration at a bolt hole can be explained in terms of the load transfer near the bolt hole during the plate is loaded. If the hole is open or contains a clearance-fit bolt, load in the plate cannot be transferred across the bolt hole but must "deflect" around the hole. This deflected portion of the load causes the stress concentration. In contrast, in the interference fitted hole, a part of the load passes through the bolt. Therefore, the hole deflects less load and consequently causes a smaller stress concentration.

The predicted crack growth lives are given in Fig. 11 for the specimens. As the figure shows at the interference fitted specimens the fatigue crack grows slowly compared to the open hole for a given crack length. This is completely appreciable for smaller crack lengths, where the interference fit has an important role in reducing the stress intensity range due to pre-stress presence. Interference fit process reduces the stress intensity factor range at the tip of the crack emanated from the hole by creating pre-stress field around the hole which leads to subsequent reduction in crack growth rate and increase in propagation life.

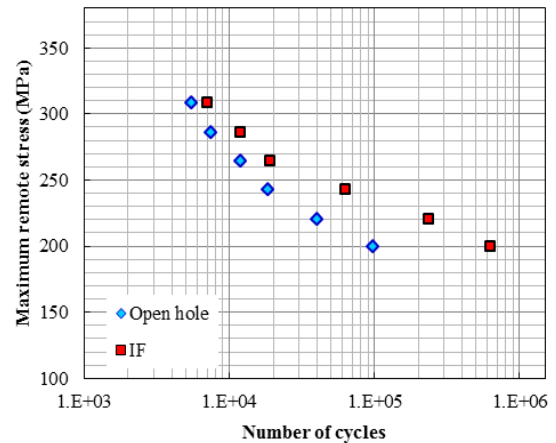


Fig. 10 The crack initiation life prediction

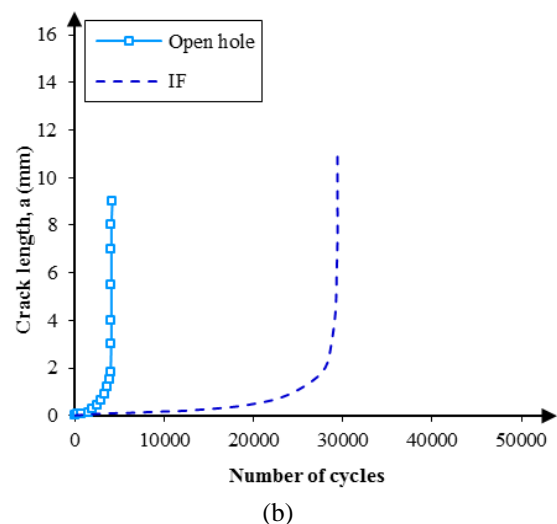
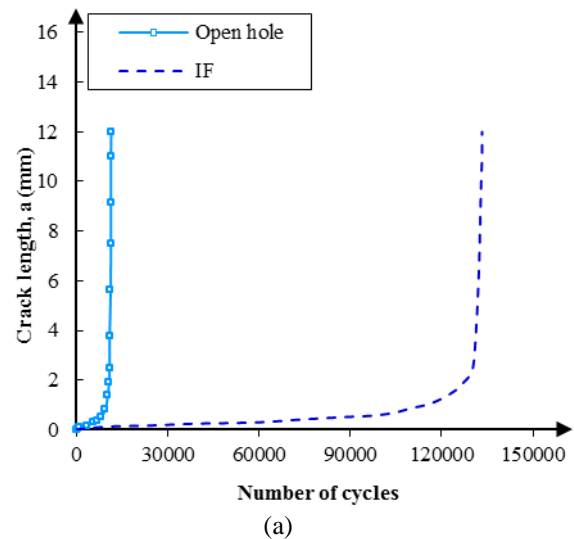


Fig. 11 Estimated of fatigue crack growth life (a) load 50 kN (b) load 60 kN

The total fatigue lives from the addition of the crack initiation and the crack propagation lives are portrayed in a graph

in Fig. 12. As the figure shows there is a good agreement between the predicted numerical and experimental fatigue lives. The numerically predicted lives show that interference fit has positive effect on improving both fatigue crack initiation and fatigue crack growth lives. Also the predicted lives from the numerical method versus the experimental results are presented in Fig. 13. As the figure shows the majority of the estimated lives satisfactorily lie within a 3×band around the experimental results.

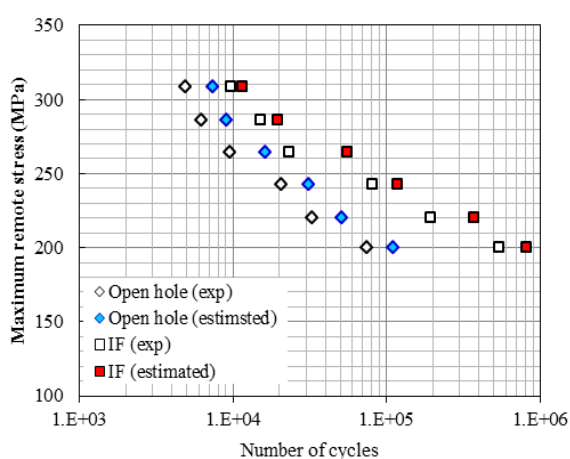


Fig. 12 S–N diagram (data) for experimental fatigue test and numerical results.

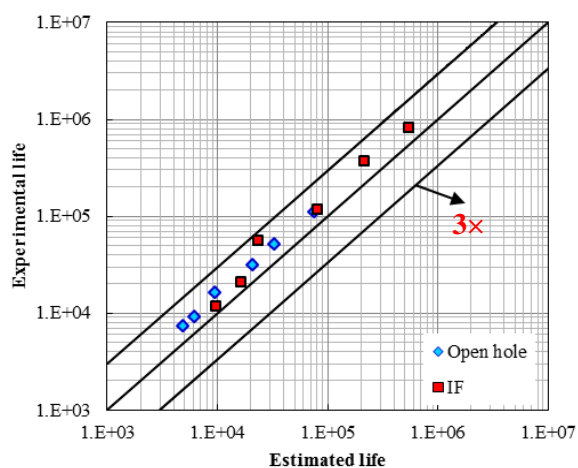


Fig. 13 Comparison between the estimated and experimental total fatigue lives.

Fig. 14 presents the fraction of estimated fatigue crack initiation and fatigue crack growth life to the estimated total fatigue life in different load levels. It is found that

in the interference fitted specimens, with increasing load level the percentage of the propagation life increases, as can be seen from Fig. 14.

In the interference fitted specimens at low level loads, a greater portion of the total life belongs to the fatigue crack initiation life. As the load level increases the percentage of the crack initiation life decreases and the portion of crack propagation life increases, so that at high level loads the percentage of the crack initiation life and crack propagation life is approximately equal (see Fig. 14). In the interference fitted specimens the percentage of initiation life varies between 50% and 77%, and the propagation life percentage varies between 23% and 50%. IF process reduces the stress intensity factor range at the tip of the crack emanated from the hole edge by creating pre-stress field around the hole which leads to the subsequent reduction in the crack growth rate and increases the propagation life. In the open hole specimens at all load levels about 72–87% of the total fatigue life belongs to the fatigue crack initiation life. In these specimens more portion of the total life is spent on the fatigue crack initiation and less portion spent on the crack propagation life (i.e. 13–28%).

To evaluate the accuracy of the method used in this research, the fatigue life estimated with this method was compared with those of the equivalent initial flaw size (EIFS) [31-33] in Fig. 15. The fatigue life of the component is assumed as the number of cycles required to propagate these initial defects until the critical dimensions.

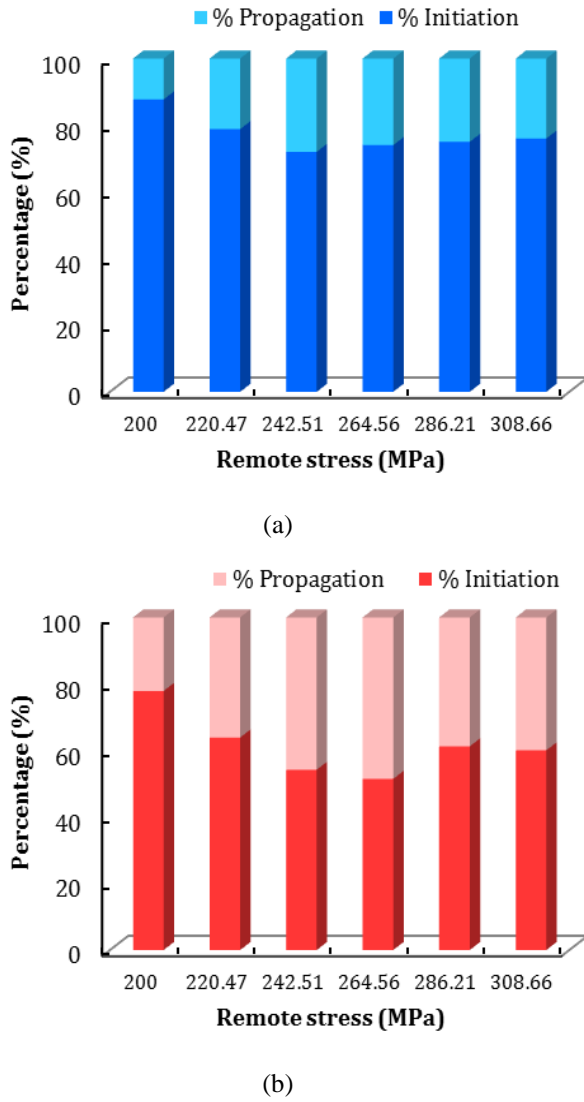


Fig. 14. The percentage of estimated total fatigue life dedicated to fatigue crack initiation and crack growth life for: (a) Open hole specimens, (b) IF specimens

The EIFS concept is a quantity extrapolated from empirical data simply to facilitate the life prediction by using long crack growth analysis and avoiding the difficulties of short crack growth modeling. In order to calculate the initial crack length in the propagation phase El Haddad [31] parameter was used:

$$a_0 = \frac{1}{\pi} \left( \frac{\Delta K_{th}}{\Delta \sigma_{fl}} \right)^2 \quad (6)$$

where  $\Delta K_{th}$  is the crack growth threshold and  $\Delta \sigma_{fl}$  is the fatigue limit. The walker crack growth law was used to predict crack propagation rate and subsequently fatigue life [28].

As the results confirm, the method used in this research shows a better agreement with the experimental test results compared with 'EIFS method'. The EIFS method underestimates the fatigue lives, though, the predicted lives are close to the two lines indicating a correlation factor of 3.

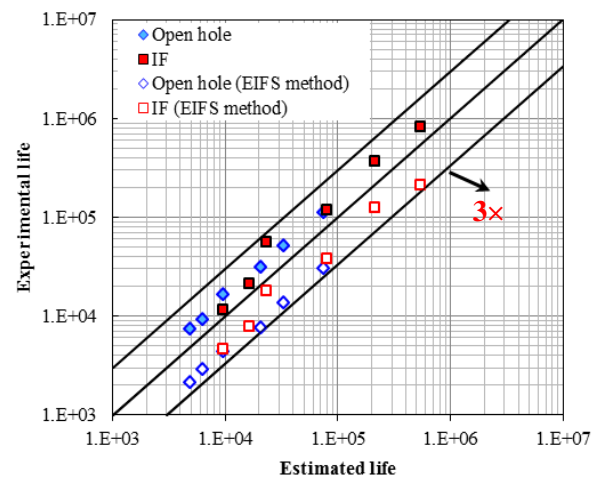


Fig. 15. Comparison between the estimated and experimental fatigue lives (no. of cycles) using two different methods.

In order to compare more quantitatively the predicted results with the experimental test results an error index has been used. The error index and mean absolute values of errors have been used as:

$$ER = \log \left( \frac{N_{Est}}{N_{Exp}} \right) \quad (7)$$

$$\overline{ER} \% = \left( \frac{1}{n} \sum_{i=1}^n |ER_j| \right) \times 100$$

where  $N_{Est}$  is the predicted life and  $N_{Exp}$  is the experimental life. The average absolute errors of the fatigue life methods are presented in Table 2. The error index shows that the error of Method used in this research is lower and therefore the

predicted life using this criterion has a lower deviation from the experimental fatigue life.

Table 2 The average absolute errors (ER%)

	Open hole	Interference fit
Method used in this research	16.12	18.96
EIFS method	37.62	28.82

### 5. Conclusions

In this paper fatigue test is conducted on AL-alloy 7075-T6 to investigate the fatigue behavior of interference fitted holes and also the fatigue life of specimens has been estimated using a numerical method. In order to obtain the pre-stress distributions due to the interference fit process, FE simulation results were used. The calculated pre-stress was used in the AFGROW computer program to predict fatigue crack propagation in the interference fitted plate. Also, the initiation life was estimated via Fatemi–Socie multiaxial fatigue criterion using the stress and strain fields obtained from the FE simulations. The numerically predicted total fatigue lives due to fatigue crack initiation and propagation were compared with the experimental fatigue test results to evaluate the capability of the numerical technique in predicting the fatigue lives.

- Fatigue tests results have shown that the interference fitted specimens endure longer fatigue life compared to the open hole specimens.
- Fractured sections of the interference fitted specimens show that fatigue crack initiates at entrance plane and propagate perpendicular to the loading

direction through the thickness. For the open hole specimens fatigue crack initiates and propagates from the mid plane at the hole edge.

- The enhanced fatigue life of the interference fitted specimens is in agreement with the relevant reduction in the level of the local mean and amplitude stresses.
- The results demonstrate that interference fit has positive influence on improving the fatigue life of both fatigue crack initiation and fatigue crack growth stages.
- The finite element results demonstrate that the pre-stress created by interference fit increases the fatigue crack initiation life by decreasing the stress concentration at the hole edge. Also the beneficial pre-stress reduces the crack stress intensity factor, therefore, increases the fatigue crack propagation life.

### References

- [1] T.N. Chakherlou, J. Vogwell, "The effect of cold expansion on improving the fatigue life of fastener holes," *Eng. Fail. Anal.*, vol. 10, 2003, pp.13–24.
- [2] Y.L. Wen, Y.L. Zhu, Sh. Hou, H. Sun, "Zhou Investigation on fatigue performance of cold expansion holes of 6061-T6 aluminum alloy," *Int. J. Fatigue*, vol. 95, 2017, pp. 216–228.
- [3] T.N. Chakherlou, R.H. Oskouei, J. Vogwell, "Experimental and numerical investigation of the effect of clamping force on the fatigue behaviour of bolted plates," *Eng. Fail. Anal.*, vol. 15. 2008, pp.563–574.
- [4] T.N. Chakherlou, H. Taghizadeh, A.B. Aghdam, "Experimental and numerical comparison of cold expansion and interference fit methods in improving

fatigue life of holed plate in double shear lap joints,” *Aero. Sci. Tech*, vol. 29, 2013, pp. 351–362.

[5] S. Kleditzsch, B. Awiszusa, M. Lätzer, E. Leidichb, “Numerical and analytical investigation of steel–aluminum knurled interference fits: Joining process and load characteristics,” *J. Mater. Process. Tech*, vol. 219, 2015, pp. 286–294.

[6] A. Mohammadpour, T.N. Chakherlou. “Numerical and experimental study of an interference fitted joint using a large deformation Chaboche type combined isotropic–kinematic hardening law and mortar contact method,” *Int. J. Mech. Sci*, vol. 106, 2016, pp.297–318.

[7] R. I. Stephens, A. Fatemi, R. Stephens, and H. O. Fuchs, “Metal Fatigue in Engineering,” John Wiley & Sons, New York, NY, USA, 2000.

[8] M.W. Brown, K.J. Miller, “A theory for fatigue failure under multiaxial stress–strain conditions,” *Proc. Instit. Mech. Eng*, vol. 187, 1973, pp.745–55.

[9] C. Ruiz, P.H.B. Boddington, K.C. Chen, “An investigation of fatigue and fretting in a dovetail joint,” *Exp Mech*, vol. 24, 1984, pp. 208–17.

[10] C.D. Lykins, S. Mall, V. Jain, “A shear stress-based parameter for fretting fatigue crack initiation,” *Fatigue. Fract. Eng. Mater. Struct*, vol. 24, 2001, pp. 461–73.

[11] D.L. McDiarmid, “A general criterion for high cycle multiaxial fatigue failure,” *Fatigue. Fract. Eng. Mater. Struct*, vol.14, 1991, pp. 429–53

[12] B. Crossland, “Effect of large hydrostatic pressures on the torsional fatigue strength of an alloy steel,” In: *Proc. Int. Conf. on fatigue of metals, institution of mechanical engineers. London; 1956*, p. 138–49.

[13] K. Smith, T. Topper, P. Watson, “A stress–strain function for the fatigue of metals (stress–strain function for metal fatigue including mean stress effect),” *J Mater* 1970;5:767–78.

[14] A. Fatemi, D.F. Socie, “A critical plane approach to multiaxial fatigue damage including out-of-phase loading,” *Fatigue. Fract. Eng. Mater. Struct*, vol. 11, 1988, pp. 149–65.

[15] J.C. Newman, E.P. Phillips, M.H. Swain, “Fatigue-life prediction methodology using small-crack theory,” *Int. J. Fatigue*, vol. 21, 1999, pp.109–19.

[16] D.V. Ramsamooj, “Analytical prediction of short to long fatigue crack growth rate using small- and large-scale yielding fracture mechanics,” *Int. J. Fatigue*, vol. 25, 2003, pp. 923–33.

[17] M. Toyosada, K. Gotoh, T. Niwa, “Fatigue crack propagation for a through thickness crack: a crack propagation law considering cyclic plasticity near crack tip,” *Int. J. Fatigue*, vol. 26, 2004, pp. 983–992.

[18] AFGROW , “Fracture mechanics and fatigue crack growth analysis software tool,” 2008;Ver 4.12.15.0.

[19] M.R. Ayatollahi, S.M.J. Razavi, H.R. Chamani, “A numerical study on the effect of symmetric crack flank holes on fatigue life extension of a SENT specimen,” *Fatigue. Fract. Eng. Mater. Struct*, vol. 37, 2014, pp.1153–1164.

[20] M.R. Ayatollahi, S.M.J. Razavi, M.Y. Yahya, “Mixed mode fatigue crack initiation and growth in a CT specimen repaired by stop hole technique,” *Fract. Eng. Mater. Struct*, vol. 145, 2015, pp.115–127.

[21] Z. Li, J. Duan, “The effect of a plastically deformed zone near crack tip on the stress intensity factors,” *Int. J. Fract* , vol. 117, 2002, pp. 29–34.

- [22] R. Zhou, P. Zhu, Z. Li, "The shielding effect of the plastic zone at mode-II crack tip," *Int. J. Fract.*, vol. 171, 2011, pp. 95–200.
- [23] J. J. Warner, P. N. Clark, D. W. Hoepfner, "Cold expansion effects on cracked fastener holes under constant amplitude and spectrum loading in the 2024-T351 aluminum alloy," *Int. J. Fatigue*, vol. 36, 2014, pp. 983–992.
- [24] D. L. Andrew, P. N. Clark, D. W. Hoepfner, "Investigation of cold expansion of short edge margin holes with pre-existing cracks in 2024-T351 aluminium alloy," *Fatigue. Fract. Eng. Mater. Struct.*, vol. 37, 2014, pp. 406–416.
- [25] E. Giner, C. Navvaro, M. Sabsabi, M. Tur, J. Dominguez, F.J. Fuenmayor, "Fretting fatigue life prediction using the extended finite element method," *Int. J. Mech, Sci*, vol. 53, 2011, pp. 217–25.
- [26] H. Taghizadeh, T.N. Chakherlou, H. Ghorbani, A. Mohammadpour. "Prediction of fatigue life in cold expanded fastener holes subjected to bolt tightening in Al alloy 7075-T6 plate," *Int. J. Mech, Sci*, vol. 90, 2015, pp. 6–15.
- [27] Swanson Analysis Systems Inc. ANSYS, Structural nonlinearities, User's Guide for Revision 13.
- [28] N. E. Dowling, *Mechanical Behavior of Materials: Engineering Methods for Deformation, Fracture, and Fatigue*: Prentice Hall, 1993.
- [29] G. Glinka and R. I. Stephens, "Total fatigue life calculations in notch SAE cast steel under variable loading spectra," *ASTM STP 791*, 1983, pp. 427–445.
- [30] R. Dhamari, "The effect of water-displacing corrosion preventives on the fatigue behaviour of mechanically fastened aluminium joints," *Ph.D. Thesis*, University of New South Wales, 2004.
- [31] Y. Xiang, Z. Lu, Y. Liu, "Crack growth-based fatigue life prediction using an equivalent initial flaw model. Part I: Uniaxial loading." *Int. J. Fatigue*, vol. 32, 2010, pp. 341–349.
- [32] H. Liu, D.-G. Shang, J.-Z. Liu, Z.K. Guo, "Fatigue life prediction based on crack closure for 6156 Al-alloy laser welded joints under variable amplitude loading," *Int. J. Fatigue*, vol. 72, 2015, pp. 11–18.
- [33] A.S.F. Alves, L.M.C.M.V. Sampayo, J.A.F.O. Correia, A.M.P. De Jesus, P.M.G.P. Moreira, P.J.S. Tavares, "Fatigue life prediction based on crack growth analysis using an equivalent initial flaw size model: Application to a notched geometry," *Proc. Eng.*, vol. 114, 2015, pp. 730 – 737.